densation with allenes provides great flexibility with respect to the substitution of the olefin in the resultant enynes, a feature not available with other condensations.[8] The simplicity and versatility of this method should make it a valuable entry to enynes and dienynes, as well as poly(enynes), useful functional building blocks and substances of growing pharmacological interest. Exploring the mechanism of this cross-condensation also represents an important avenue for future work.[9]

Acknowledgment. We thank the National Science Foundation for their generous support of our programs. We are grateful to the Deutsche Forschungsgemeinschaft for a fellowship to G.K.

Supplementary Material Available: Spectroscopic and analytical details for **1**, **2**-E, **3**, **4**-E, **7**, **8**, **10**, **13**, and **14** (5 pages). Ordering information is given on any current masthead page.

---

(8) Trost, B. M.; Chan, C.; Ruhter, G. *J. Am. Chem. Soc.* **1987**, *109*, 3486.

(9) In a typical experimental procedure, the terminal acetylene and allene in an approximately 1:1 ratio was added to a solution of 3 mol % of either TCPC or palladium acetate and 3 mol % of the ligand in benzene to create a solution that was approximately 0.2–0.3 M in substrates. After stirring at 50–60 °C until the starting material disappeared, evaporation and chromatographic separation gave the purified products.

On the Anomaly of the Metal–Carbon Bond Strength in $(CH_3)_2M$ Compounds of the Heavy Elements M = Au^-, Hg, Tl^+, and Pb^{2+}. Relativistic Effects in Metal–Ligand Force Constants

Peter Schwerdtfeger[†]

Department of Chemistry and the Center of
Information Science, University of Auckland
Private Bag, Auckland, New Zealand

Received September 7, 1989

In this paper attention is drawn to the fact that relativistic effects are important in force constants involving heavy metal-ligand bonds. The trend in the metal–carbon bond strength in dimethyl complexes of the Hg, Tl, and Pb follows an unexpected order,[1] Figure 1. The metal–carbon stretching force constants in the isoelectronic series MMe_2 (M = Cd, In^+, and Sn^{2+}; Me = CH_3) increase from the left to the right due to the increasing nuclear charge, i.e., $k_e(CdMe_2) < k_e(InMe_2^+) < k_e(SnMe_2^{2+})$. In contrast, a decrease is observed for the heavy metal series, $k_e(HgMe_2) > k_e(TlMe_2^+) > k_e(PbMe_2^{2+})$.[2,3] The unusually large k_e(M–C) has been discussed in terms of 5d participations in the M–C bond[1,3-8] or due to the possibility of hydration effects on the positively charged species.[2] However, the origin of this anomaly still remains unknown. It has been suggested recently[5] that the unusually large force constant in $HgMe_2$ may be attributed to relativistic effects. Relativistic effects in force constants have not been studied extensively.[9,10] In the series Au, Hg, Tl, and Pb the relativistic 6s-orbital contraction decreases from the left to the right ("Au-maximum"; see ref 9). Hence, we expect the largest relativistic change in molecular properties in $AuMe_2^-$ and the smallest in $PbMe_2^{2+}$. This would explain the anomaly in force constants discussed above. This communication shows that the decrease in M–C force constants from $HgMe_2$ to $TlMe_2^+$ is due to relativistic effects, whereas the decrease from $TlMe_2^+$ to $PbMe_2^{2+}$ is also revealed at the nonrelativistic level.

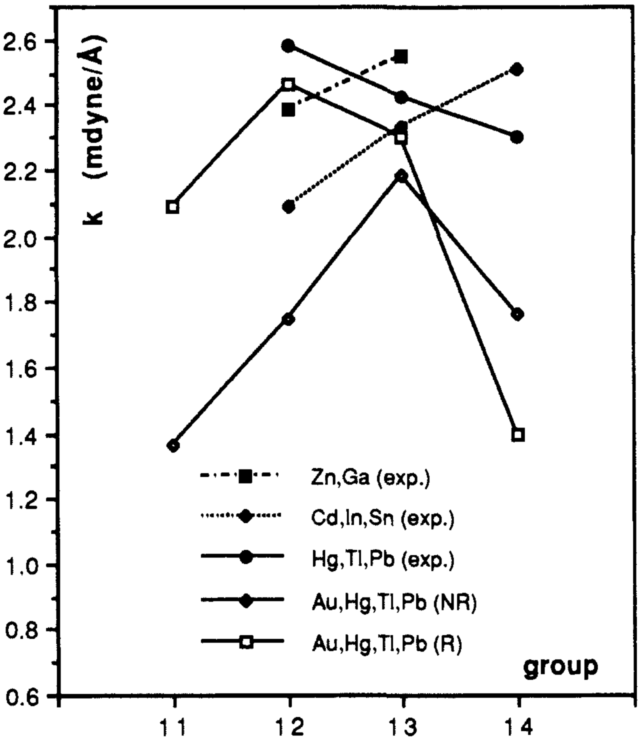

Figure 1. Variation of the metal–carbon stretching force constants in the isoelectronic series $ZnMe_2$, $GaMe_2^+$, $CdMe_2$, $InMe_2^+$, $SnMe_2^{2+}$, $HgMe_2$, $TlMe_2^+$, and $PbMe_2^{2+}$ taken from generalized valence force fields (refs 2, 3, and 20). The experimental force constant for $GaMe_2^+$ has been estimated from ref 2.

To solve this long-standing problem, nonrelativistic (NR) and relativistic (R) Hartree–Fock (HF) calculations using multi-electron adjusted spin-orbit averaged pseudopotentials for gold, mercury, thallium, and lead have been performed for $AuMe_2^-$, $HgMe_2$, $TlMe_2^+$, and $PbMe_2^{2+}$.[11] The HF geometries have been optimized.[11,12] The M–C bond distances and symmetric stretching force constants have been derived from a second-order Møller–Plesset perturbation method (MP2)[11,12] The basis sets and pseudopotentials are described in refs 5, 13, 14, and 15.

The MP2 metal–carbon bond lengths and symmetric stretching force constants are in close agreement with the latest experimental results (Table I). The largest relativistic change in r_e(MC) and $k_e(M\text{–}CH_3)$ has been calculated for $AuMe_2^-$, Table II. It is evident that relativity is the reason for the anomaly in the metal–carbon bond strength of mercury and thallium; i.e., the nonrelativistic calculated force constants show the expected increase as obtained for the methyl complexes of the elements in the fifth (and possibly of the fourth) period of the periodic table, Figure

---

[†] Present address: Research School of Chemistry, The Australian National University, G.P.O. Box 4, Canberra, A.C.T. 2601, Australia.

(1) Goggin, P. L. Ph.D. Thesis, Oxford, 1960.

(2) Hobbs, Ch. W.; Tobias, S. *Inorg. Chem.* **1970**, *9*, 1998.

(3) (a) Miles, M. G.; Patterson, J. H.; Hobbs, C. W.; Hopper, M. J.; Overend, J.; Tobias, R. S. *Inorg. Chem.* **1968**, *7*, 1721. (b) Freidline, C. E.; Tobias, R. S. *Inorg. Chem.* **1966**, *5*, 354.

(4) Adams, D. M. In *Metal-Ligand and Related Vibrations*; Edward Arnold: London, 1967; p 206.

(5) Schwerdtfeger, P.; Boyd, P. D. W.; Bowmaker, G. A.; Mack, H. G.; Oberhammer, H. *J. Am. Chem. Soc.* **1989**, *111*, 15. Compare also scattered wave Xα relativistic (nonrelativistic) gross atomic 5d-orbital populations for $Tl(CH_3)_2^+$ 9.95 (10.00), $Hg(CH_3)_2$ 9.76 (9.89), and $Au(CH_3)_2^-$ 9.51 (9.54) (Schwerdtfeger, P.; Boyd, P. D. W.; Bowmaker, G. A. Unpublished Results). Xα calculations by DeKock et al. (ref 6) also showed that 5d excitations in the $Hg(CH_3)_2$ photoelectron spectra are atomic-like.

(6) DeKock, R. L.; Baerends, E. J.; Boerrigter, P. M.; Hengelmolen, R. *J. Am. Chem. Soc.* **1984**, *106*, 3387.

(7) Hall, J. R. In *Essays in Structural Chemistry*; Downs, A. J., Leng, D. A., Staveley, L. A. K., Eds.; Macmillan: London, 1971; p 437.

(8) Maslowsky, E. *Vibrational Spectra of Organometallic Compounds*; Wiley: New York, 1977.

(9) Pyykkö, P. *Chem. Rev.* **1988**, *88*, 563.

(10) Schwerdtfeger, P. Thesis, Stuttgart, 1985.

(11) (a) Frisch, M. J.; Binkley, J. S.; Schlegel, H. B.; Raghavachari, K.; Melius, C. F.; Martin, L.; Stewart, J. J. P.; Bobrowicz, F. W.; Rohlfing, C. M.; Kahn, L. R.; DeFrees, D. J.; Seeger, R.; Whiteside, R. A.; Fox, D. J.; Fluder, E. M.; Pople, J. A. program GAUSSIAN86, Carnegie-Mellon Quantum Chemistry Publishing Unit: Pittsburgh, PA, 1984. Extended for local and nonlocal pseudopotentials by P. Schwerdtfeger using program PSEPOT for the latter: Kolar, M. *Comp. Phys. Commun.* **1981**, *23*, 275. (b) Pople, J. A.; Seeger, R.; Krishnan, R. *Int. J. Quant. Chem. Symp.* **1977**, *11*, 149.

(12) For $HgMe_2$ a basis set of 169 primitive Gaussians contracted to 109 basis functions has been used. A HF geometry optimization required about 25 h CPU time on a IBM3081 computer. A one-point MP2 (CISC) calculation required about 2 (30) h CPU time.

0002-7863/90/1512-2818$02.50/0

Table I. Molecular Properties for the MMe_2 ($M = Au^-$, Hg, Tl^+, and Pb^{2+})[l]

molecule	method	$r_e(MC)^a$	$r_e(CH)$	$\alpha_e(MCH)$	$D_e(M-CH_3)^a$	$k_e(M-CH_3)^a$	$q(M)$	$q(C)$	n_p
$AuMe_2^-$	NR	2.290	1.095	111.6	324 (−71)	1.265	0.43	−0.97	0.16
	R	2.142	1.095	111.8	401 (+6)	2.094	0.08	−0.54	0.19
	exp	2.124^b							
$HgMe_2$	NR	2.248	1.087	110.9	299 (−96)	1.746	0.80	−0.84	0.86
	R	2.104	1.086	110.7	286 (−109)	2.462	0.60	−0.75	0.43
	exp	2.094^c	1.09^c	109.3^c	234^d	$2.410,^e$ 2.58^f			
$TlMe_2^+$	NR	2.187	1.083	109.7	333 (−62)	2.187	1.32	−0.83	0.59
	R	2.082	1.081	109.0	304 (−91)	2.305	1.20	−0.79	0.43
	exp	2.097^g				$2.204,^h$ 2.43^i			
$PbMe_2^{2+}$	NR	2.213	1.084	106.7	465 (+70)	1.764	1.61	−0.67	0.85
	R	2.197	1.083	104.7	406 (+11)	1.395	1.38	−0.55	0.87
	exp	$2.238,^j$ 2.30^k	1.083^j			2.30^i			

[a] MP2 values. [b] From $AuMePPh_3$, ref 16. [c] Reference 17. [d] Reference 18. [e] Reference 19. [f] Reference 20. [g] Reference 21. [h] Reference 22. [i] Reference 2. [j] From $PbMe_4$, ref 23. [k] Reference 3 (assumed). [l] Bond distances r_e in Å, M–C–H angles in deg, dissociation energies $D_e(M(CH_3)_2 \rightarrow M + 2CH_3)$ in kJ/mol (in brackets $D_e(M(CH_3)_2 \rightarrow M + C_2H_6)$), symmetric $M-CH_3$ stretching force constants k_e ($k_r + k_{rr}$; see ref 19) in mdyne/Å, Mulliken gross atomic charges $q(M)$ and $q(C)$, and metal 6p populations n_p.

Table II. Relativistic Effects in the Dimethyl Complexes of Au, Hg, Tl, and Pb[a]

molecule	$\Delta_R r_e(MC)$	$\Delta_R D_e$-$(M-CH_3)$	$\Delta_R k_e$-$(M-CH_3)$	$\Delta_R q(M)$
$AuMe_2^-$	0.148	−77	−0.829	0.35
$HgMe_2$	0.144	+13	−0.716	0.20
$TlMe_2^+$	0.105	+29	−0.118	0.12
$PbMe_2^{2+}$	0.016	+59	+0.369	0.23

[a] $\Delta_R r_e(MC)$ in Å, $\Delta_R D_e(M-CH_3)$ in kJ/mol and $\Delta_R k_e(M-CH_3)$ in mdyne/Å (see Table I).

1. However, $PbMe_2^{2+}$ has a very small nonrelativistic bond strength and shows a further relativistic decrease in $k_e(Pb-CH_3)$. To test the accuracy of the approximations used, the relativistic pseudopotential for lead given by Durand[24] has been used that leads to almost the same results (MP2; $r_e(Pb-C) = 2.213$ Å, $k_e(Pb-CH_3) = 1.482$ mdyne/Å, $D_e = 437$ kJ/mol). In addition, configuration interaction calculations with single and double substitutions corrected by size consistency effects (CISC) do not change the trends shown in Figure 1 ((NR) $r_e(Pb-C) = 2.237$ Å, $k_e(Pb-CH_3) = 1.533$ mdyne/Å; (R) $r_e(Pb-C) = 2.232$ Å, $k_e(Pb-CH_3) = 1.139$ mdyne/Å). The relativistic bond contraction at the CI level is only 0.005 Å. It was suggested recently[15] that due to the relativistic bond contraction the nuclear–nuclear repulsion increases, resulting in an overall increase in the metal–ligand stretching force constants. This effect is certainly small in $PbMe_2^{2+}$ which may explain the reverse trend in the relativistic change of the $Pb-CH_3$ stretching force constant ($\Delta_R k_e > 0$; Table II). Also electronic effects are important by increasing the overlap and therefore the bond strength.[8] The increasing p participation in the metal–carbon bonds from Au to Pb (Table I) is directly correlated to the decrease in $\Delta_R r_e(MC)$; i.e., the p-orbitals only slightly contract due to relativistic effects and therefore quench the relativistic 6s contraction.[10] The large 6p participation in $PbMe_2^{2+}$ may suggest a $^3E'$ (D_{3h}) ground state with an open shell $Pb(\sigma^1\pi^1)$ occupation, but this state is about 3.6 eV (HF, vertical transition) above the $^1A'$ state. Also a linear C–Pb–C arrangement has been obtained (MP2: $k_\alpha(C-Pb-C) = 0.063$ mdyne/Å). Hence, the vibrational spectrum obtained for $PbMe_2^{2+}$ given in ref 2 does not correspond to the free two-coordinated linear species $PbMe_2^{2+}$.

Klemperer pointed out the nonmonotonic behavior in force constants of the group(12) halides.[25] Also a nonmonotonic behavior in the M–C force constants of the group(12) methyl complexes was found by Miles et al.:[3] $ZnMe_2$, 2.38; $CdMe_2$, 2.05; $HgMe_2$, 2.46 mdyne/Å (NR/MP2: 1.75 mdyne/Å). The same trend is seen in the metal–carbon bond lengths measured by Rao et al.:[17] $ZnMe_2$, 1.929, $CdMe_2$, 2.112; $HgMe_2$, 2.094 Å (NR/MP2; value 2.248 Å). To study the importance of correlating the 5d electrons, the 5d orbitals have been excluded from the active MP2 orbital range. The results for $HgMe_2$ are as follows: (NR) $r_e(Hg-C) = 2.306$ Å, $k_e(Hg-CH_3) = 1.651$ mdyne/Å, $D_e = 257$ kJ/mol; (R) $r_e(Hg-C) = 2.187$ Å, $k_e(Hg-CH_3) = 1.856$ mdyne/Å, $D_e = 189$ kJ/mol. Relativistic CISC calculations confirm these values (5d active: $r_e(Hg-C) = 2.103$ Å, $k_e(Hg-CH_3) = 2.478$ mdyne/Å; 5d inactive: $r_e(Hg-C) = 2.199$ Å, $k_e(Hg-CH_3) = 1.742$ mdyne/Å). The CI values are in close agreement with the MP2 results. The Hg–C bond distances are larger, and the $Hg-CH_3$ force constants are smaller without 5d correlation (compared to Table I), but the relativistic increase in $k_e(Hg-CH_3)$ is remarkably small (29%). Furthermore, at the HF level the $Hg-CH_3$ stretching force constant is decreasing due to relativistic effects, i.e., $k_e(Hg-CH_3) = 1.687$ mdyne/Å (NR) and $k_e(Hg-CH_3) = 1.371$ mdyne/Å (R). Hence, 5d correlation is very important for the relativistic increase in $k_e(Hg-CH_3)$; i.e., the relativistic 6s contraction makes the Hg(5d) electrons more accessible. Obviously, this is not the case for $TlMe_2^+$, where the energy gap between the 5d and 6s orbitals is larger compared to $HgMe_2$. Within a good approximation the 5d electrons may be regarded as core-like. Similar effects have been obtained for $AuMe_2^-$ (MP2, 5d inactive: (NR) $r_e(Au-C) = 2.405$ Å, $k_e(Au-CH_3) = 0.836$ mdyne/Å, $D_e = 144$ kJ/mol; (R) $r_e(Au-C) = 2.195$ Å, $k_e(Au-CH_3) = 1.663$ mdyne/Å, $D_e = 200$ kJ/mol).

The increase in oxidation state from +I ($AuMe_2^-$) to +IV ($PbMe_2^{2+}$) is reflected nicely in the increase in the Mulliken gross metal charges, Table I. The relativistic increase in electronegativity ($\Delta_R EN(Au) = -0.4$[13]), is also reflected in q(M). An updated table of electronegativities[26] shows a nonmonotonic behavior due to the relativistic 6s contraction,[13] Cu 1.90, Ag 1.72, Au 2.22, Zn 1.76, Cd 1.71, Hg 1.83. Durig and Brown related this trend in electronegativities to the nonmonotonic behavior in the group(12) metal–carbon bond distances of the methyl complexes.[27] This turns out to be clearly a relativistic effect due to the relativistic 6s contraction.

---

(13) Schwerdtfeger, P.; Dolg, M.; Schwarz, W. H. E.; Bowmaker, G. A.; Boyd, P. D. W. *J. Chem. Phys.* **1989**, *91*, 1762.

(14) (a) Schwerdtfeger, P. *Phys. Scr.* **1987**, *36*, 453. (b) Schwerdtfeger, P.; Silberbach, H.; Miehlich, B. *J. Chem. Phys.* **1989**, *90*, 762. (c) Dolg, M.; Andrea, D. Private communication.

(15) Schwerdtfeger, P.; Boyd, P. D. W.; Burrell, A. K.; Robinson, W. T.; Taylor, M. J. *Inorg. Chem.* In press.

(16) Gavens, P. D.; Grey, J. J.; Mays, M. J.; Sheldrick, G. M. *Acta Crystallogr.* **1980**, *B33*, 137.

(17) Rao, K. S.; Stoicheff, B. P.; Turner, R. *Can. J. Phys.* **1960**, *38*, 1516.

(18) Elschenbroich, Ch.; Salzer, A. *Organometallics* VCH Publ.: New York, 1986.

(19) Mink, J.; Gellai, B. *J. Organomet. Chem.* **1974**, *66*, 1.

(20) Bakke, K. A. M. W. *J. Mol. Spectrosc.* **1972**, *41*, 1.

(21) Hughes, D. L.; Turner, M. R. *Acta Crystallogr.* **1983**, *B39*, 329.

(22) Schwerdtfeger, P.; Bowmaker, G. A.; Boyd, P. D. W.; Ware, D. C.; Brothers, P. J.; Nielson, A. J. *Organometallics*. In press.

(23) Oyamada, T.; Iijima, T.; Kimura, M. *Bull. Chem. Soc. Jpn.* **1971**, *44*, 2638.

(24) Barthelat, J. C.; Pelessier, M.; Villemur, P.; Devilliers, R.; Trinquier, G.; Durand, Ph., Program PSHONDO(PSATOM), Toulouse, 1981.

(25) Klemperer, W. *J. Chem. Phys.* **1956**, *25*, 1066.

(26) Nepela, D. A.; McKay, J. M. *Physica C* **1989**, *158*, 65.

(27) Durig, J. R.; Brown, S. C. *J. Mol. Spectrosc.* **1973**, *45*, 338.

Spin-orbit effects have been neglected for the MP2 dissociation energies, since these are assumed to be small for these compounds.[5,13] Only $AuMe_2^-$ shows a relativistic increase in the dissociation energy. The trend in dissociation energy is opposite to the trend in force constants discussed above, i.e., $D_e(HgMe_2) > D_e(TlMe_2^+) > D_e(PbMe_2^{2+})$. The dissociation energy of $C_2H_6 \rightarrow 2CH_3$ has been calculated to be 395 kJ/mol at the MP2 level (exp 368 kJ/mol[28]). According to the reaction $[M(CH_3)_2]^n \rightarrow M^n + C_2H_6$ (e.g., $n = -1$ for M = Au), the methyl complexes are not very stable at the relativistic level (Table I). Also entropy effects clearly would shift the reaction to the right hand side. This agrees with the fact that Hg–C bonds in organomercury compounds can be easily broken homolytically. On the other hand, such compounds are relatively air- and water-resistant and therefore kinetically stable. The calculated MP2 dissociation energy for $HgMe_2$ of 286 kJ/mol is in relatively good agreement with the experimental value of 234 kJ/mol.

Acknowledgment. The author is indebted to the Alexander von Humboldt Stiftung for financial support and to IBM New Zealand Ltd. for providing computer time. Thanks are due to M. Dolg basis sets and pseudopotentials and to Prof. Warren R. Roper and Prof. Michael J. Taylor for carefully reading of this paper.

---

(28) Streitwieser, A.; Heathcock, C. H. *Introduction to Organic Chemistry*; Macmillan: New York, 1981.

Observation of a Peroxyl Radical in Samples of "Purple" Lipoxygenase[1]

Mark J. Nelson* and Rebecca A. Cowling

Central Research and Development Department
E. I. du Pont de Nemours and Company
Wilmington, Delaware 19880-0328

Received December 18, 1989

We report the existence of a peroxyl radical, analogous to a proposed mechanistic intermediate, in samples of the metastable purple form of soybean lipoxygenase-1. This enzyme[2] catalyzes the production of 13-hydroperoxy-9,11-*cis,trans*-octadecadienoic acid (13-HPOD[3]) from linoleic acid. Mammalian lipoxygenases catalyze similar reactions of arachidonic acid and are important in the production of leukotrienes and lipoxins, messengers involved in the inflammatory and immune responses.[4] One hypothetical mechanism of the oxygenation reaction, similar to that of the autoxidation of polyunsaturated fatty acids,[5] proposes that the active-site Fe^{3+} oxidizes the 1,4-diene unit of the substrate to a pentadienyl radical, which should react smoothly with dioxygen, giving a peroxyl radical.[6] Reduction by the iron (now Fe^{2+}) would result in the peroxide anion. A second mechanism proposes that the Fe^{3+} facilitates the deprotonation of the substrate, yielding a Fe^{3+}–alkyl complex. Insertion of dioxygen into the Fe–C bond, then, is envisioned as giving the coordinated peroxide anion.[7] Radicals derived from the substrate have been trapped in experiments in which the reaction is prevented from going to completion by anaerobiasis.[8] However, such radicals may result from homolytic Fe–C bond cleavage of the proposed Fe^{3+}–alkyl complex as well as from simple release of free-radical intermediates.[7] Recently, broad EPR spectra consistent with fatty acid peroxyl radicals were reported in samples of lipoxygenase under turnover conditions at room temperature.[9] In that case, the peroxyl radical was thought to be in solution, rather than enzyme-bound, and thus conclusions of mechanistic relevance are somewhat tenuous.

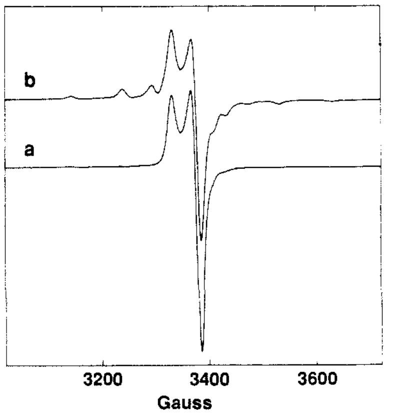

Figure 1. EPR spectra of "purple" lipoxygenase generated by addition of linoleic acid under oxygen. (a) Natural-abundance O_2. (b) 36% enriched $^{17}O_2$. Samples prepared as stated in the text. EPR parameters: microwave frequency, 9.52 GHz; power, 1 mW; modulation amplitude, 0.5 mT; temperature, 10 K.

Treatment of ferric soybean lipoxygenase-1 with 13-HPOD or with linoleic acid and oxygen results in the formation of a metastable purple enzyme.[10] This form reverts slowly to the native ferric enzyme with release of 12,13-epoxy-11-hydroxy-9-octadecanoic acid,[11] suggesting that it represents an intermediate complex on the isomerization pathway. The origin of the purple color, endowed by a band in the visible spectrum at 585 nm, has never been adequately explained, but CD spectra suggest that the environment of the metal ion is significantly different in the native ferric and purple states.[12]

EPR spectra[13] of purple lipoxygenase prepared by treating ferrous or ferric lipoxygenase[14] with linoleic acid in the presence of oxygen at 4 °C show an axial signal in the $g = 2$ region (Figure 1a). When the experiments were repeated with 36% ^{17}O-enriched

---

(1) Contribution No. 5223.

(2) Veldink, G. A.; Vliegenthart, J. F. G. *Adv. Inorg. Biochem.* **1984**, *6*, 139-163.

(3) Abbreviation: 13-HPOD, 13-hydroperoxy-9,11-*cis,trans*-octadecadienoic acid.

(4) Samuelsson, B. E.; Dahlén, S.-E.; Lindgren, J. A.; Rouzer, C. A.; Serhan, C. N. *Science* (*Washington, D.C.*) **1987**, *237*, 1171-1176.

(5) Porter, N. A. *Acc. Chem. Res.* **1986**, *19*, 262-268.

(6) Petersson, L.; Slappendel, S.; Vliegenthart, J. F. G. *Biochim. Biophys. Acta* **1985**, *828*, 81-85.

(7) Corey, E. J.; Nagata, R. *J. Am. Chem. Soc.* **1987**, *109*, 8107-8108.

(8) De Groot, J. J. M. C.; Garssen, G. J.; Vliegenthart, J. F. G.; Boldingh, J. *Biochim. Biophys. Acta* **1973**, *326*, 279-284. Conner, H. D.; Fischer, V.; Mason, R. P. *Biochem. Biophys. Res. Commun.* **1986**, *141*, 614-621.

(9) Chamulitrat, W.; Mason, R. P. *J. Biol. Chem.* **1989**, *264*, 20968-20973.

(10) De Groot, J. J. M. C.; Garssen, G. J.; Veldink, G. A.; Vliegenthart, J. F. G.; Boldingh, J.; Egmond, M. R. *FEBS Lett.* **1975**, *56*, 50-54. Egmond, M. R.; Fasella, P. M.; Veldink, G. A.; Vliegenthart, J. F. G.; Boldingh, J. *Eur. J. Biochem.* **1977**, *76*, 469-479.

(11) Garssen, G. J.; Veldink, G. A.; Vliegenthart, J. F. G.; Boldingh, J. *Eur. J. Biochem.* **1976**, *62*, 33-36. Corey, E. J.; Mehrotra, M. M. *Tetrahedron Lett.* **1983**, *24*, 4921-4922.

(12) Spaapen, L. J. M.; Veldink, G. A.; Liefkens, T. J.; Vliegenthart, J. F. G.; Kay, C. M. *Biochim. Biophys. Acta* **1979**, *574*, 301-311.

(13) EPR spectra were obtained at the X band on a Bruker EM200 spectrometer using an Air Products LTR-3 cryostat. Field positions were measured with a calibrated Hall probe gaussmeter and microwave frequencies with an HP5342a microwave frequency meter. Spectra were integrated by using a Bruker ESP 1600 computer and compared to a Cu(EDTA) standard. Simulations were performed by using ESRa (Calleo Scientific Software Publishers) on an Apple Macintosh II computer.

(14) Soybean lipoxygenase-1 was purified and assayed as published;[15] the enzyme used had specific activities between 250 and 270 units/mg. Stock solutions of linoleic acid (Sigma Chemical Co.) were prepared by evaporating an ethanolic solution to an oil under N_2, then redissolving in 0.1 volume of 1 M NH_4OH, and adding 0.9 volume of 0.1 M sodium borate, pH 9. Concentrated ferrous or ferric lipoxygenase was diluted into oxygen-saturated buffer in a serum-stoppered cuvette thermostated at 4 °C in an HP4150a diode-array spectrophotometer. The spectrum was obtained after each aliquot of linoleic acid was added. Addition was terminated after the absorption at 585 nm no longer increased upon further addition of substrate. Samples were transferred with chilled syringes to EPR tubes on ice and rapidly frozen in liquid nitrogen.

(15) Nelson, M. J. *Biochemistry* **1988**, *27*, 4273-4278.

0002-7863/90/1512-2820$02.50/0